Construction of Two Inorganic-organic Hybrid Vanadogermanates Based on Di-Cd-Substituted Ge-V-O Cluster and Transition-metal Complex Bridges

RU Jing-Jing[1,2] (茹晶晶);GU Ya-Nan[1] (顾亚男);MA Xiang[1] (马祥);CHEN Jian-Zhong[1] (陈建中);ZHENG Shou-Tian[1] (郑寿添);LI Xin-Xiong[1] (李新雄)

[1] *College of Chemistry, Fuzhou University, Fuzhou* 350116, *China*;[2]*Department of Chemistry, Ningde Normal University, Ningde, Fujian* 352100, *China*

ABSTRACT Two new inorganic-organic hybrid vanadogermanates H[Cd(en)(phen)(H_2O)][Cd(en)(phen)]{[Cd(phen)]$_2$[$Ge_8V_{12}O_{41}(OH)_7$]} 5H_2O (**1**) and [Cd(dien)$_2$][Cd(dien)]$_2${[Cd(phen)]$_2$$Ge_8V_{12}O_{42}$($H_2O$)$(OH)_6$} 6.5$H_2O$ (**2**) (en = ethylenediamine, dien = diethylenetriamine, phen = 1,10-phenanthroline) have been synthesized by hydrothermal method. Their structures were measured by single-crystal X-ray diffractions, thermogravimetric analysis, powder X-ray diffractions and infrared spectra. Structural analysis reveals that compound **1** is an infrequent dimeric structure based on di-Cd-substituted Ge-V-O cluster and transition-metal complex bridges, while compound **2** is an infinite 1-D chain constructed from di-Cd-substituted Ge-V-O clusters and dinuclear bridging complexes. Magnetic measurement indicated that both **1** and **2** exhibit antiferromagnetic behaviors.

Keywords: vanadogermanates; hydrothermal synthesis; crystal structure; magnetic property;
DOI: 10.14102/j.cnki.0254-5861.2011-1741

1 INTRODUCTION

Nowadays, more and more researchers are interested in polyoxometalates (POMs) because of their superior properties in catalysis, optics, magnetism, sorption, ion exchange and so on[1-4]. Compared with polyoxomolybdates and polyoxotungstates, polyoxovanadates (POVs) are less investigated relatively[5-8]. The most important characteristic in polyoxovanadate compounds is that there are various polyhedron construction units such as {VO_4}, {VO_5}, {VO_6} and so on, which can form different vanadium-oxygen clusters through sharing vertexes, edges and planes. One of the most effective approaches for the development of POVs is the incorporation of heteroatoms into the clusters. Up to now, most studies focus on the incorporation of group 15 elements (As, Sb) into the well-known Keggin {$V_{18}O_{42}$} cluster anion, which are named as

vanadoarsenates[9-15] and vanadoantimonates[16-21]. The $\{As_2O_5\}/\{Sb^{III}_2O_5\}$ dimers are formed by two vertex-sharing $\{AsO_3\}/\{SbO_3\}$ trigonal pyramids, which substitute the VO_5 groups on the $\{V_{18}O_{42}\}$ shell. Compared with vanadoarsenates and vanadoantimonates, the research of vanadosilicates(VSOs) and vanadogermanates(VGOs) is relatively scarce. The germanium-vanadium oxide clusters based on $\{V_{18}O_{42}\}$ shell mainly include $\{Ge_4V_{16}O_{46}\}$ cluster[7, 22], $\{Ge_6V_{15}O_{48}\}$ cluster[23-24], $\{Ge_8V_{14}O_{50}\}$ cluster[7, 24] and $\{Ge_8V_{12}O_{48}\}$ cluster[7]. These clusters are mainly made up of $\{VO_5\}$ square pyramids and $\{Ge_2O_7\}$ dumbbell dimers. The $\{Ge_2O_7\}$ units are formed by two vertex-sharing $\{GeO_4\}$ tetrahedra, which are superior to the trigonal pyramid of $\{AsO_3\}$ and $\{SbO_3\}$. The $\{AsO_3\}$ and $\{SbO_3\}$ trigonal pyramids usually tend to form isolated structures because of the weak coordination capability of As/Sb^{III} lone pairs[25-27].

It is well known that the second transition-metal(TM) ions incorporated into POVs skeletons may produce attractive structures and some special properties. But, fewer investigations have been carried out on TM-substituted POVs. Up to now, there are only a few cases such as $\{[(en)_2Cd_2Ge_8V_{12}O_{40}(OH)_8(H_2O)][Cd(en)_2]_2\}\ 6H_2O$[23] reported in 2010, $\{(CdX)_4Ge_8V^{IV}_{10}O_{46}(H_2O)[V^{III}(H_2O)_2]_4(GeO_2)_4\}\ 8H_2O$ (X = en, 1,2-dap)[28] reported by Yang's group at 2014 and $\{[Cd(en)_2][Cd(en)]_2Ge_8V_{12}O_{40}(OH)_8\}_2\{[Cd(en)(H_2O)]_2\}$ en $2H_2O$[29] made by Liu's group at 2016. Recently, our group have reported two novel transition-metal substituted vanadogermanates $[Cd(en)(H_2O)_2][Cd(en)_2][Cd(en)]\{[Cd(en)]_2[Ge_8V_{12}O_{42.5}(OH)_5]\}\ 2H_2O$ and $[Cd(en)_3][Cd(en)]_2\{[Cd(en)]_2[Ge_8V_{12}O_{42}(OH)_6]\}\ 10H_2O$[30]. Inspired by this result, we decide to further explore this system.

In this work, we report the hydrothermal syntheses, crystal structures and magnetic properties of another two new transition-metal substituted vanadogermanates $H[Cd(en)(phen)(H_2O)][Cd(en)(phen)]\{[Cd(phen)]_2[Ge_8V_{12}O_{41}(OH)_7]\}\ 5H_2O$ (**1**) and $[Cd(dien)_2][Cd(dien)]_2\{[Cd(phen)]_2Ge_8V_{12}O_{42}(H_2O)(OH)_6\}\ 6.5H_2O$ (**2**). **1** is an uncommon dimeric structure based on di-Cd-substituted Ge-V-O cluster and transition-metal complex bridges. **2** exhibits an infinite 1-D chain structure built by di-Cd-substituted Ge-V-O clusters and dinuclear bridging complexes.

2 EXPERIMENTAL

2. 1 Materials and measurements

All chemicals with analytical grade were purchased from commercial sources without any further purification. Elemental analyses of C, H and N were carried out with a Vario EL III elemental analyzer. Powder X-ray diffraction (PXRD) patterns of the samples were measured by a computer automated diffractometer (Bruker D8 Advance) equipped with Cu-$K\alpha$ radiation (λ = 1.54056 Å) at room temperature with 2θ values from 5 to 50 ° at a step of 0.02 °. Fourier transform infrared (FT-IR) spectroscopy (4000～400 cm^{-1}) were recorded on a Nicoletis 10 spectrometer with KBr pellets. Thermogravimetric (TG) analysis was examined in the temperature of 20～1000 °C at a heating rate of 10 °C/min under flowing N_2 atmosphere on a NETZSCH PC409 simultaneous thermal analyzer. The magnetic susceptibility data were measured with a Quantum Design MPMS SQUID VSM magnetometer in an external magnetic field of 1 KOe at 2～300 K.

2. 2 Synthesis

During our exploration, we found that some factors including pH value, temperature and reaction time can affect the formation and crystal growth of the final products. Lots of parallel experiments prove that crystals of **1** and **2** were sensitive to the pH values of the reaction. The optimal pH values for crystal growth are 8.8～9.0 for **1** and 8.5～8.8 for **2,** respectively. What's more, the reaction temperature plays a vital role in the formation **1** and **2**. When the reaction temperature was adjusted out of 160～180 ºC, **1** and **2** can not be obtained. Finally, the best reaction time should be in 3～5 days.

2. 2. 1 Synthesis of 1

A mixture of NH_4VO_3 (0.0345 g, 0.29 mmol), GeO_2 (0.0384 g, 0.37 mmol), $CdCl_2·2.5H_2O$ (0.0242 g, 0.11 mmol), phen (0.0306 g, 0.17 mmol), en (0.1 mL) and H_2O (5 mL) was stirred for 0.5 h. Then it was transferred to a 25 mL Teflon-lined stainless-steel autoclave and sealed. The mixture was heated at 170 ℃ for 4 days and then cooled to room temperature. Brown block-shaped crystals were recovered by filtration, washed with distilled water, and dried at ambient temperature (Yield: 0.0711 g, 46% on the base of GeO_2). Elemental analysis (%) calcd. for $H_{68}C_{52}N_{12}O_{54}V_{12}Ge_8Cd_4$ (3366.97): C, 18.55; N, 4.99; H, 2.02. Found (%): C, 18.30; N, 5.01; H, 2.33. IR (KBr, cm^{-1}): 3438(s), 3275(w), 3048(w), 1617(m), 1574(m), 1516(m), 1427(s), 1350(w), 1145(w), 1103(w), 984(s), 793(s), 729(m), 668(m), 542(m).

2. 2. 2 Synthesis of 2

A mixture of NH_4VO_3 (0.0200 g, 0.17 mmol), GeO_2 (0.0380 g, 0.36 mmol), $CdCl_2·2.5H_2O$ (0.0800 g, 0.35 mmol), phen (0.0300 g, 0.17 mmol), dien (0.2 mL) and H_2O (5 mL) was stirred for 0.5 h. Then it was

transferred to a 25 mL Teflon-lined stainless-steel autoclave and sealed. The mixture was heated at 170 ℃ for 4 days and then cooled to room temperature. Brown block-shaped crystals were recovered by filtration, washed with distilled water, and dried at ambient temperature (Yield: 0.0448 g, 29% based on GeO_2). Elemental analysis (%) calcd. for $H_{89}C_{40}N_{16}O_{55.5}V_{12}Ge_8Cd_5$ (3436.44): C, 13.98; N, 6.52; H, 2.59. Found (%): C, 14.01; N, 6.57; H, 2.98. IR (KBr, cm^{-1}): 3422(w), 3352 (w), 3276(w), 2924(w), 2876(w), 1589(m), 1516(m), 1426(m), 1341(w), 1143(w), 1101(w), 984(s), 790(s), 728(w), 669(m), 552(m).

2. 3 Single-crystal X-ray crystallography

X-ray diffraction data for **1** and **2** were collected on a Bruker APEX II CCD diffractometer at 296(2) K equipped with a fine focus, 2.0 kW sealed tube X-ray source (Mo$K\alpha$ radiation, λ = 0.71073 Å) operating at 50 kV and 30 mA. The empirical absorption correction was based on equivalent reflections. The structures were solved by direct methods and refined on F^2 by full-matrix least-squares methods using the SHELXS-97 and SHELXL-97 programs, respectively. All hydrogen atoms attached to carbon, nitrogen and oxygen atoms were geometrically placed. All non-H atoms were refined anisotropically except O7w, O8w and O9w in compound **1**. The final formulas of **1** and **2** were determined by single-crystal X-ray diffraction together with elemental analysis and thermogravimetric analysis. Meanwhile, to balance the charge of **1**, one proton should be added. The proton cannot be located and it was assumed to be delocalized on the overall structure, which is often observed in POM chemistry. All these crystal data and structure refinement details are summarized in Table 1.

Table 1. Crystal Data and Structure Refinement for 1 and 2

Compound	**1**	**2**
Empirical formula	$H_{68}C_{52}N_{12}O_{54}V_{12}Ge_8Cd_4$	$H_{89}C_{40}N_{16}O_{55.5}V_{12}Ge_8Cd_5$
Formula weight	3366.97	3436.44
Temperature/K	296(2)	296(2)
Crystal system	Triclinic	Monoclinic
Space group	$P\bar{1}$	$C2/c$
a/Å	14.5015(12)	16.978
b/Å	16.6199(13)	24.183
c/Å	23.1666(18)	26.542
α/ °	71.4930(10)	90
β/ °	84.2940(10)	99.18
γ/ °	75.4820(10)	90
Volume/Å^3	5124.5(7)	10758.4
Z	2	8
ρ_{calc}mg/mm^3	2.173	2.186
F(000)	3214	6808

Reflns collected	31867	22280
Unique reflns (R_{int})	17724 (0.0177)	9463(0.0243)
Restraints/parameters	18/1291	36/652
GOOF on F^2	0.995	1.040
Final *R* indices ($I > 2\sigma(I)$)	$R = 0.0635$, $wR = 0.2038$	$R = 0.0564$, $wR = 0.1586$
R indices (all data)	$R = 0.0779$, $wR = 0.2440$	$R = 0.0740$, $wR = 0.1747$

$R = \sum||F_o| - |F_c||/\sum|F_o|$, $wR = [\sum w(F_o^2 - F_c^2)^2/\sum w(F_o^2)^2]^{1/2}$; $w = 1/[\sigma^2(F_o^2) + (xP)^2 + yP]$,

where $P = (F_o^2 + 2F_c^2)/3$. $x = 0.1852$ and $y = 65.1392$ for **1**; $x = 0.0942$ and $y = 185.5212$ for **2**

3 RESULTS AND DISCUSSION

3. 1 Crystal structure of 1

Single-crystal X-ray diffraction analyses reveal that **1** crystallizes in triclinic $P\bar{1}$ space group and its molecular structure consists of one di-Cd-substituted Ge-V-O cluster $\{[Cd(phen)]_2[Ge_8V_{12}O_{41}(OH)_7]\}^{5-}$ (**1a**), one decorative $[Cd(en)(phen)(H_2O)]^{2+}$ group, one $[Cd(en)(phen)]^{2+}$ fragment and five lattice water molecules. As shown in Fig. 1a-1b, an unusual feature of **1a** is that two $[Cd(phen)]^{2+}$ groups take the place of two VO^{2+} groups located between the Ge_2O_7 units of the reported $\{Ge_8V_{14}O_{42}(OH)_8\}$ polyanion with rhombicuboctahedral topology[31], generating a new $\{Cd_2Ge_8V_{12}O_{40}(OH)_8\}$ cluster, which belongs to α-$\{Ge_8V_{12}O_{40}(OH)_8\}$ configuration[30]. Each **1a** cluster is further decorated by one $[Cd(phen)(en)(H_2O)]^{2+}$ group to form the unprecedented cluster $\{[Cd(phen)(en)(H_2O)][Cd(phen)]_2[Ge_8V_{12}O_{41}(OH)_7]\}^{3-}$. In **1**, four unique Cd^{2+} ions exhibit two different coordination environments: trigonal prisms CdO_4N_2 (Cd(1), Cd(2)) and distorted octahedral CdO_2N_4 (Cd(3), Cd(4)). The Cd(1) and Cd(2) ions in **1a** are coordinated by two N atoms of one phen ligand and four bridging O atoms from two adjacent VO_5 tetragonal pyramids of **1a**. Different from Cd(1) and Cd(2), both Cd(3) and Cd(4) are chelated by two different kinds of nitrogen-containing organic ligands. For Cd(4), it is defined by one O atom of VO_5 polyhedron, one coordinated water molecule, one en ligand and one phen ligand. For Cd(3), it is surrounded by one en ligand, one phen molecule and two O atoms (Fig. 1c), forming a $[CdO_2(en)(phen)]$ fragment. It should be noted that one of the two O atoms in the $[CdO_2(en)(phen)]$ fragment is from a GeO_4 tetrahedron (O(27)) in **1a**, and the other O atom from a VO_5 tetragonal pyramid (O(11)) from a neighboring symmetry-related **1a** cluster. In **1**, all V centers have a distorted VO_5 square-pyramidal environment. The V-O bond lengths of terminal O atoms vary from 1.588(8) to 1.633(7) Å, and the bridging O atoms fall in the 1.903(7)~2.015(7) Å range. The Ge-O distances range from 1.708(7) to 1.781(8) Å. On the basis of bond valence sum (BVS) calculations[32], the oxidation states of all V atoms are +4

(3.96~4.31), and also +4 (3.95~4.06) for all Ge atoms in **1** (Table 2). In addition, the BVS calculations for terminal O atoms (O(2), O(5), O(6), O(9), O(12), O(15), O(20)) connected with Ge atoms are in the range of 0.99~1.08, which suggests that these O atoms belong to OH groups. The most interesting structure feature of **1** is that the [Cd(en)(phen)(H_2O)] decorated **1a** clusters can be interconnected by two [CdO_2(en)(phen)] fragments to give rise to a dimeric aggregate (Fig. 1d). Though some POM dimeric compounds based on POM building blocks bridged by transition-metal complexes have been reported[29], the dimeric aggregate containing mixed ligands chelated transition complexes is infrequent. Therefore, the occurrence of **1** not only enriches the dimeric POM chemistry, but also provides a feasible synthetic method for gathering more vanadogermanate clusters to poly(vanadogermanate)s aggregates.

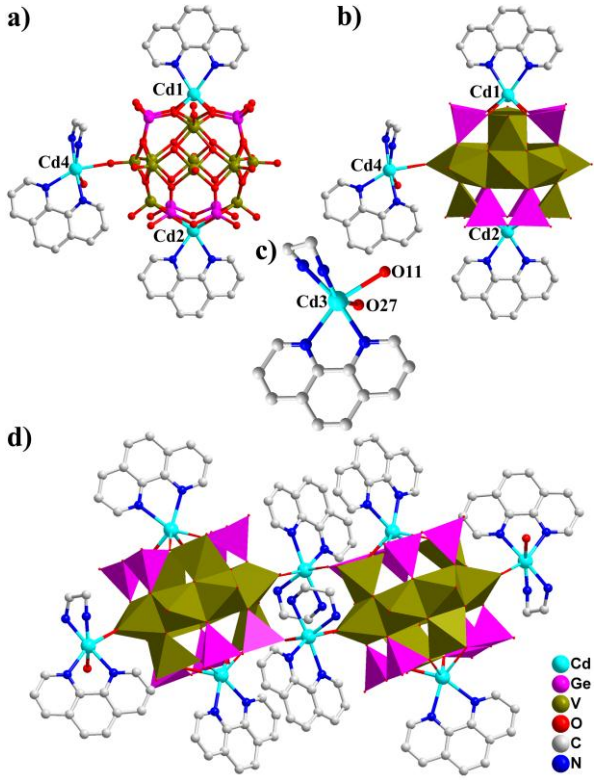

Fig. 1. a)-b) Ball and stick and polyhedral representations of [Cd(en)(phen)(H_2O)]{[Cd(phen)]$_2$[$Ge_8V_{12}O_{41}(OH)_7$]}$^{3-}$ cluster in 1; c) Structure of bridging complex [CdO_2(en)(phen)]$^{2-}$; d) View of the dimeric structure of 1.

All hydrogen atoms are omitted for clarity. Color codes: GeO_4, purple; VO_5, olive

Table 2. Bond Valence Sum Calculation for 1

Atoms	Bond valence (III)	Bond valence (IV)	Bond valence (V)
V(1)	3.97	4.19	3.96
V(2)	4.00	4.22	3.99
V(3)	3.90	4.10	3.88
V(4)	3.91	4.12	3.90
V(5)	3.88	4.09	3.88
V(6)	3.98	4.19	3.96
V(7)	3.83	4.03	3.82
Atoms	Bond valence	Atoms	Bond valence
Ge(1)	4.02	O(H)(3)	1.01
Ge(2)	4.09	O(H)(21)	1.03
Ge(3)	4.02	O(H)(24)	1.03
Ge(4)	4.06		

3. 2 Crystal structure of 2

The molecular structure of **2** contains one di-Cd-substituted Ge-V-O cluster $\{[Cd(phen)]_2[Ge_8V_{12}O_{41}(OH)_6]\}^{6-}$ (**2a**, Fig. 2a-2b), one $[Cd(dien)_2]^{2+}$ group, two $[Cd(dien)]^{2+}$ units and 6.5 lattice water molecules. The structure and configuration of **2a** are similar to those of **1a** except the number of hydroxyl groups on the cluster. The number of hydroxyl groups in **2a** is six, while that of **1a** is seven. The Ge–O/V–O bond distances for the terminal O atoms fall in the ranges of 1.706(1)~1.743(2)/1.593(8)~1.616(5) Å, and those for the bridging O atoms are in the ranges of 1.713(3)~1.799(1)/1.923(2)~2.009(4) Å. On the basis of BVS calculations (Table 3), the oxidation states of all V are +4 (4.03~4.22), and those of all Ge atoms are +4 (4.02~4.09) in **2**. Three unique Cd^{2+} ions (Cd(1), Cd(2), Cd(3)) within **2** exhibit three different coordination geometries: distorted trigonal bipyramid CdO_2N_3 for Cd(1), trigonal prisms CdO_4N_2 for Cd(2) and pentagonal bipyramid $CdON_6$ for Cd(3). The Cd(1) ion is composed of three N atoms of one dien ligand (Cd–N: 2.269(8)~2.416(8) Å) and two μ_3-O atoms of GeO_4 tetrahedron from two neighboring **2a** clusters. Interestingly, two symmetry-related Cd(1) ions are interconnected through sharing two μ_3-O atoms, leading to the formation of a dinuclear complex $[Cd_2O_2(en)_2(phen)_2]$ with centrosymmetry (Fig. 2c). The Cd(2) ion is defined by two N atoms of one phen ligand (Cd–N 2.339(7)~2.410(8) Å) and four μ_3-O of **2a** cluster (Cd–O: 2.264(5)~2.331(6) Å). Cd(3) is surrounded by six N atoms of two dien ligands (Cd–N: 2.380(1)~2.47(2) Å) and one O atom of a VO_5 tetragonal pyramid of **2a** (Cd–O: 2.618(9) Å), forming a decorative $[CdO(dien)_2]$ unit mounted on the exterior of **2a** cluster. Worth a mention is the further assembly of **2a** clusters. As depicted in Fig. 2c, each 2a cluster linked two neighboring ones by two dinuclear complexes $[Cd_2O_2(dien)_2]$ through sharing Ge–O–Cd bonds, leading to the formation of an infinite 1-D chain (Fig. 2d). The successful

construction of such 1-D chain further proved that tetragonal {GeO_4} groups are superior to the trigonal pyramid of {AsO_3} and {SbO_3} in building extended polyoxovanadate structures.

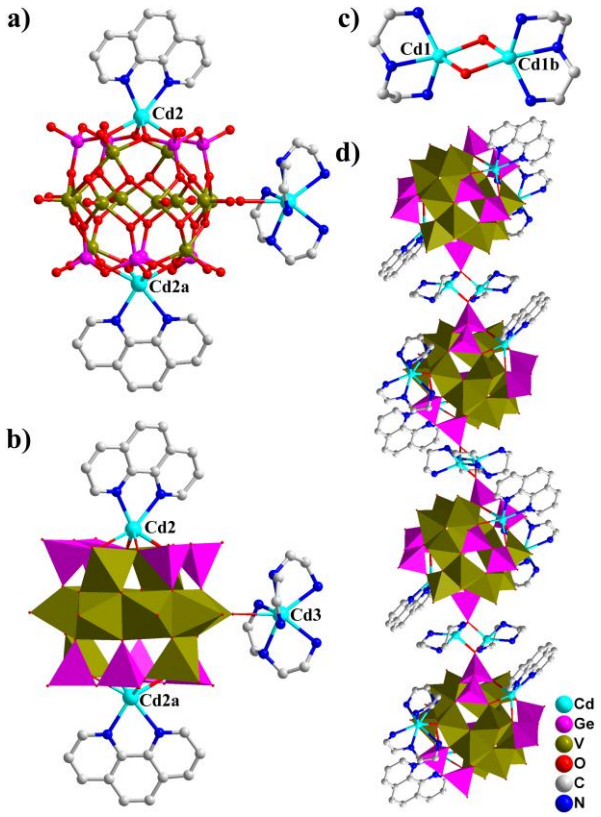

Fig. 2. a) and b) Ball and stick/polyhedral representations of {[Cd(phen)]$_2$[$Ge_8V_{12}O_{42}(OH)_6$]}$^{6-}$ cluster in 2; c) View of the dinuclear bridging complex [Cd_2(dien)$_2O_2$]; d) View of the 1-D chain in 2. All hydrogen atoms are omitted for clarity. Symmetric codes: a: 1–*x*, *y*, 0.5–*z*; b: 1.5–*x*, –0.5–*y*, 1–*z*

Table 3. Bond Valence Sum Calculations for 2

Atoms	Bond valence (III)	Bond valence (IV)	Bond valence (V)
V1	3.97	4.19	3.96
V2	4.00	4.22	3.99
V3	3.90	4.10	3.88
V4	3.91	4.12	3.90
V5	3.88	4.09	3.88
V6	3.98	4.19	3.96
V7	3.83	4.03	3.82
Atoms	Bond valence	Atoms	Bond valence
Ge1	4.02	O(H)3	1.01
Ge2	4.09	O(H)21	1.03
Ge3	4.02	O(H)24	1.03
Ge4	4.06		

3. 3 PXRD analysis

In the PXRD patterns of **1** and **2** (Fig. 3), the good accordance between the experimental patterns and the simulated ones indicates good phase purities.

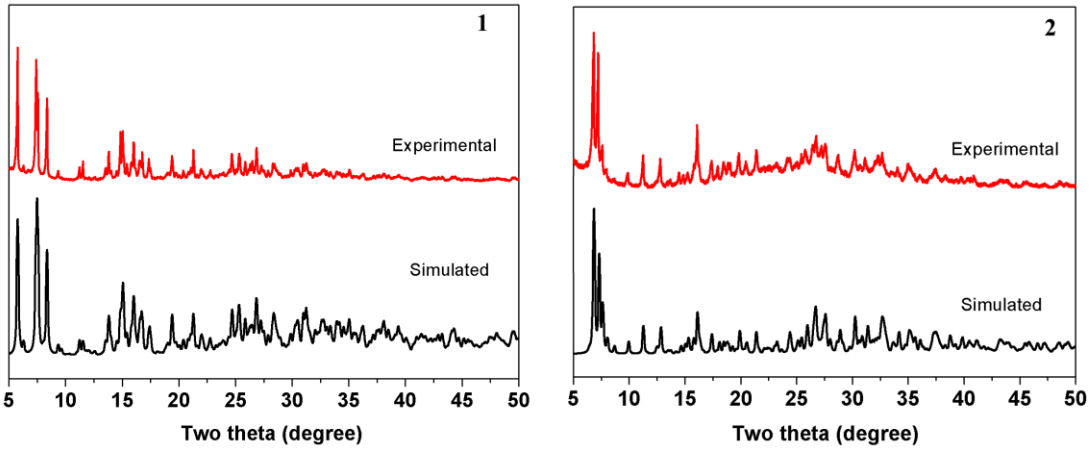

Fig. 3. Experimental and simulated PXRD patterns of 1 and 2

3. 4 FT-IR analysis

IR spectra of **1** and **2** are shown in Fig. 4. The NH_2 and CH_2 stretching bands are observed at 3383～3312 and 2975～2890 cm^{-1}, and the absorption peaks at 1609～1570 cm^{-1} can be attributed to the NH_2 bending bands. These signals confirm the presence of amino groups in **1** and **2**. The broad band at 3462～3391 cm^{-1} can result from the OH stretching. The peaks lying in 1536～1401 and 738～705 cm^{-1} can be assigned to the phen ligand. The strong peaks situated in 1016～896 cm^{-1} belong to the stretching vibrations of V=O bonds, whereas those at 879～743 cm^{-1} may be due to the Ge–O stretching vibration of the GeO_4 tetrahedra[23]. The peaks located at 2386～2289 cm^{-1} are attributed to the asymmetric stretching vibration of CO_2.

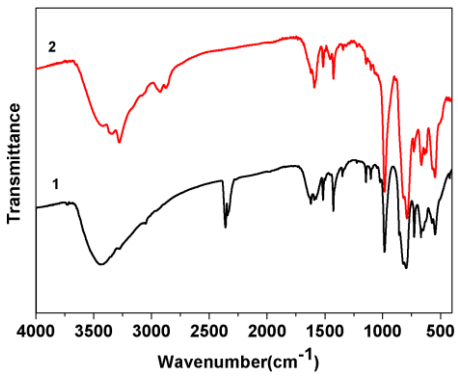

Fig. 4. IR spectra of 1 and 2

3. 5 TG analysis

The TGA curves of **1** and **2** are shown in Fig. 5. For **1**, a weight loss of 5.92% in the range of 20～300 ºC observed corresponds to the removal of five H_2O molecules and two en ligands (calcd: 6.24%). The second weight loss about 4.40% from 300 to 500 ºC is assigned to the removal of seven hydroxyl groups and one coordinated water ligand (calcd: 4.06%). Then the weight loss about 21.27% from 500 to 813 ºC is caused by the decomposition of four phen molecules (calcd.: 21.38%). For **2**, the weight loss of 7.87% from 20 to 125 ºC is due to the departure of 7.5 water molecules and removal of six hydroxyl groups (calcd: 6.90%). The weight loss of 11.23% from 125 to 415 ºC results from the loss of four dien molecules (calcd: 12.01%). After that, a sequence of weight loss about 10.49% from 415 to 585 ºC can be attributed to the decomposition of two phen ligands (calcd: 10.50%).

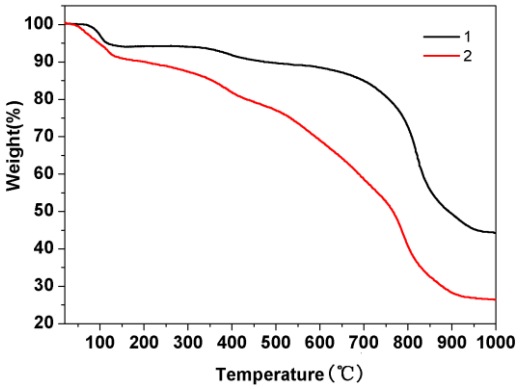

Fig. 5. TG curves of 1 and 2

3. 6 Magnetic properties

The variable-temperature magnetic susceptibilities of **1** and **2** have been measured in the temperature range of 2～300 K with an external field of 1 KOe (Figs. 6 and 7). At room temperature, the experimental $\chi_m T$ values of **1** and **2** are 1.36 and 1.36 cm^3 K mol^{-1} per formula unit respectively, much lower than the theoretical value of 4.5 cm^3 K mol^{-1} for twelve uncoupled V^{4+} ions considering g = 2.00. Upon cooling, the $\chi_m T$ values of **1** and **2** decrease slowly to 1.08 cm^3 K mol^{-1} at 48 K and 1.25 cm^3 K mol^{-1} at 35 K. On cooling, the $\chi_m T$ values of **1** and **2** decrease abruptly, reaching the minima of 0.07 and 0.09 cm^3 K mol^{-1} at 2 K. The above behaviors suggest the presence of antiferromagnetic coupling with the cluster in **1** and **2**[33]. From the structural stand point of view, the bond length between the V ··V pairs with double O bridges fall in the ranges of 2.852~3.025 Å for **1** and 2.847~3.027 Å for **2**, which are expected for antiferromagnetic coupling[23, 34]. Additionally, the temperature dependence of the reciprocal susceptibility ($1/\chi_m$) obeys the Curie-Weiss law in the temperature range of 220 to 9 K and 245 to 5 K for **1** and **2**, respectively. The Weiss and Curie constants

are –8.61 K and 1.26 $cm^3 \cdot K \cdot mol^{-1}$ for **1** and –1.07 K and 1.27 $cm^3 \cdot K \cdot mol^{-1}$ for **2**, which further support the presence of antiferromagnetic interactions between the V^{4+} ions within the clusters. Therefore, antiferromagnetic properties are observed in the two compounds that are not unexpected.

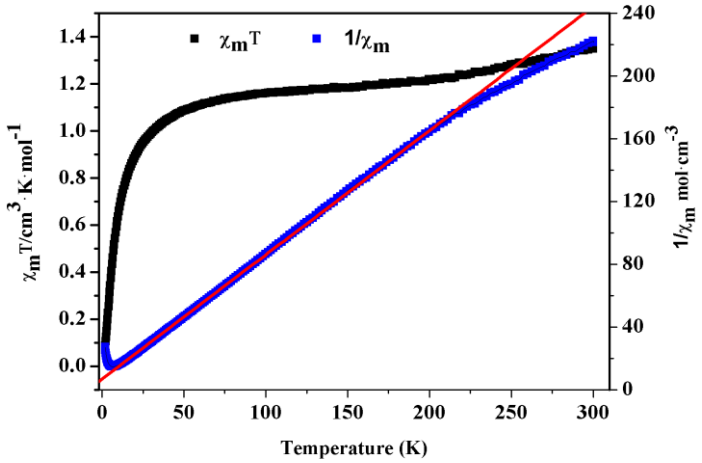

Fig. 6. Temperature dependence of $\chi_m T$ and $1/\chi_m$ for 1 between 2 and 300 K

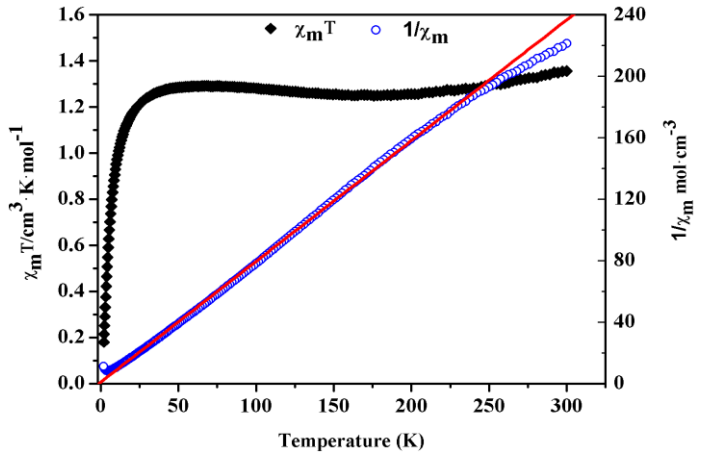

Fig. 7. Temperature dependence of $\chi_m T$ and $1/\chi_m$ for 2 between 2 and 300 K

4 CONCLUSION

We have successfully constructed two new inorganic-organic hybrid vanadogermanates under hydrothermal conditions. Structural analysis reveals that compound **1** is an infrequent dimeric structure based on di-Cd-substituted Ge–V-O cluster $[Cd(en)(phen)(H_2O)]\{[Cd(phen)]_2[Ge_8V_{12}O_{41}(OH)_7]\}^{3-}$ and transition-metal complex $[CdO_2(en)(phen)]^{2-}$ bridges, while compound **2** is an infinite 1-D chain constructed from di-Cd-substituted Ge–V-O cluster $\{[Cd(phen)]_2[Ge_8V_{12}O_{42}(OH)_6]\}^{6-}$ and dinuclear complex $[Cd_2(dien)_2O_2]$ bridges. Magnetic studies indicate that **1** and **2** have antiferromagnetic coupling between the metal ions within the clusters. This work not only enriches the structural diversity of inorganic-organic hybrid

vanadogermanates, but also confirms the great potential for making novel functional materials by linking discrete transition-metal substituted Ge–V–O clusters with various transition-metal complex bridges.

REFERENCES

(1) Wang, L.; Li, W. X.; Ye, D. D.; Gu, X. M.; Shan, Y. X.; Ni, L. Synthetic assembly of inorganic-organic polyoxometalate hybrid structures employing noncovalent interactions between 5,6-substituted 1,10-phenanthroline derivative ligands. *Chin. J. Struct. Chem.* **2016**, 35, 1655–1665.

(2) Wei, K. Y.; Yang, T.; Qin, S. J.; Ma, X.; Li, X. X.; Yang, G. Y. Hydrothermal synthesis, structural characterization and proton-conducting property of a 3-D framework based on Zr_3Na_3-substituted polyoxometalate building blocks. *Chin. J. Struct. Chem.* **2016**, 35, 1461–1468.

(3) Zhang, Z. X.; Sadakane, M.; Murayama, T.; Sakaguchi, N.; Ueda, W. Preparation, structural characterization, and ion-exchange properties of two new zeolite-like 3D frameworks constructed by ε-keggin-type polyoxometalates with binding metal ions, $H_{11.4}[ZnMo_{12}O_{40}Zn_2]^{1.5-}$ and $H_{7.5}[Mn_{0.2}Mo_{12}O_{40}Mn_2]^{2.1-}$. *Inorg. Chem.* **2014**, 53, 7309–7318.

(4) Li, X. X.; Wang, Y. X.; Wang, R. H.; Cui, C. Y.; Tian, C. B.; Yang, G. Y. Designed assembly of heterometallic cluster organic frameworks based on Anderson-type polyoxometalate clusters. *Angew. Chem. Int. Ed.* **2016**, 55, 6462–6466.

(5) Ou, G. C.; Yuan, X. Y.; Li, Z. Z. The first example of inorganic-organic compound involving the largest vanadium cluster of $[V_{34}O_{82}]^{10-}$: hydrothermal synthesis and characterization of a one-dimensional chain of $\{[NiC_{16}H_{36}N_4]_5[V_{34}O_{82}]\}_n$. *Chin. J. Struct. Chem.* **2013**, 32, 375–380.

(6) You, L. S.; Zhu, Q. Y.; Zhang, X.; Pu, Y. Y.; Bian, G. Q.; Dai, J. A new type of germanium-vanadate cluster, $[Ge_5V_6O_{21}(heda)_6]$ (Hheda = N-(2-hydroxyethyl)ethylenediamine). *CrystEngComm*. **2013**, 15, 2411–2415.

(7) Whitfield, T.; Wang, X.; Jacobson, A. J. Vanadogermanate cluster anions. *Inorg. Chem.* **2003**, 42, 3728–3733.

(8) Ou, G. C.; Liao, Y.; Xiang, Y. F.; Yuan, X. Y.; Li, Z. Z. Syntheses and structures of three hybrid materials using vanadium polyoxoanions and macrocyclic copper complex as building blocks. *Chin. J. Struct. Chem.* **2017**, 36, 135–142.

(9) He, X. L.; Liu, Y. P.; Gong, K. N.; Han, Z. G.; Zhai. X. L. Copper-organic cationic ring with an inserted arsenic-vanadium polyanionic cluster for efficient catalytic Cr^{VI} reduction using formic acid. *Inorg. Chem.* **2015**, 54, 1215–1217.

(10) Shi, S. Y.; Chen, Y.; Xu, J. N.; Zou, Y. C.; Cui, X. B.; Wang, Y.; Wang, T. G.; Xu, J. Q.; Gao, Z. M. Zero- and two-dimensional structures based on As^{III}-V^{IV} polyoxometalates. *CrystEngComm*. **2010**, 12, 1949–1954.

(11) Zheng, S. T.; Zhang, J.; Li, B.; Yang, G. Y. The first solid composed of $\{As_4V_{16}O_{42}(H_2O)\}$ clusters. *Dalton Trans.* **2008**, 5584–5587.

(12) Qi, Y. F.; Li, Y. G.; Wang, E. B.; Zhang, Z. M.; Chang, S. Metal-controlled self-assembly of arsenic-vanadium-cluster backbones with organic ligands. *Dalton Trans.* **2008**, 2335–2345.

(13) Zhou, J.; Zheng, S. T.; Fang, W. H.; Yang, G. Y. A new 2-D network containing $\{As_4V_{16}O_{42}(H_2O)\}$ cluster units. *Eur. J. Inorg. Chem.* **2009**, 2009, 5075–5078.

(14) Zheng, S. T.; Chen, Y. M.; Zhang, J.; Xu, J. Q.; Yang, G. Y. Hybrid inorganic-organic 1D and 2D frameworks with $[As_6V_{15}O_{42}]^{6-}$ polyoxoanions as building blocks. *Eur. J. Inorg. Chem.* **2006**, 2006, 397–406.

(15) Zheng, S. T.; Zhang, J.; Yang, G. Y. $[\{Zn(enMe)_2\}_2(enMe)_2\{Zn_2As_8V_{12}O_{40}(H_2O)\}]\cdot 4H_2O$: a hybrid molecular material based on covalently linked inorganic Zn-As-V clusters and transition metal complexes via enMe ligands. *Eur. J. Inorg. Chem.* **2004**, 2004, 2004–2007.

(16) Hu, X. X.; Xu, J. Q.; Cui, X. B.; Song, J. F.; Wang, T. G. A novel one-dimensional framework material constructed from antimony-substituted polyoxovanadium clusters: $[(C_2N_2H_{10})_2\beta\text{-}\{Sb^{III}_8V^{IV}_{14}O_{42}(H_2O)\}](C_2N_2H_8)\cdot 4H_2O$. *Inorg. Chem. Commun.* **2004**, 7, 264–267.

(17) Lühmann, H.; Näther, C.; Kögerler, P.; Bensch, W. Solvothermal synthesis and crystal structure of a heterometal-bridged $\{V_{15}Sb_6\}$ dimer: $[Ni_2(tren)_3(V_{15}Sb_6O_{42}(H_2O)_{0.5})]_2[Ni\text{-}(trenH)_2]\cdot H_2O$. *Inorg. Chim. Acta* **2014**, 421, 549–552.

(18) Wutkowski, A.; Näther, C.; Kögerler, P.; Bensch, W. $[V_{16}Sb_4O_{42}(H_2O)\{VO(C_6H_{14}N_2)_2\}_4]$: a terminal expansion to a polyoxovanadate archetype. *Inorg. Chem.* **2008**, 47, 1916–1918.

(19) Antonova, E.; Näther, C.; Bensch, W. Assembly of $[V_{15}Sb_6O_{42}(H_2O)]^{6-}$ cluster shells into higher dimensional aggregates via weak Sb-N/Sb-O intercluster interactions and a new polyoxovanadate with a discrete $[V_{16}Sb_4O_{42}(H_2O)]^{8-}$ cluster shell. *CrystEngComm*. **2012**, 14, 6853–6859.

(20) Antonova, E.; Näther, C.; Kögerler, P.; Bensch, W. Expansion of antimonato polyoxovanadates with transition metal complexes: $(Co(N_3C_5H_{15})_2)_2[\{Co(N_3C_5H_{15})_2\}V_{15}Sb_6O_{42}(H_2O)]\cdot 5H_2O$ and $(Ni(N_3C_5H_{15})_2)_2[\{Ni\text{-}(N_3C_5H_{15})_2\}V_{15}Sb_6O_{42}(H_2O)]\cdot 8H_2O$. *Inorg. Chem.* **2012**, 51, 2311–2317.

(21) Antonova, E.; Wutkowski, A.; Näther, C.; Bensch, W. New antimonato polyoxovanadates based on the $[V_{14}^{IV}Sb_8^{III}O_{42}(H_2O)]^{4-}$ cluster type. *Solid State Sci.* **2011**, 13, 2154–2159.

(22) Gao, Y. Z.; Xu, Y. Q.; Huang, K. L.; Han, Z. G.; Hu, C. W. Two three-dimensional $\{V_{16}Ge_4\}$-based open frameworks stabilized by diverse types of Co^{II}-amine bridges and magnetic properties. *Dalton Trans.* **2012**, 41, 6122–6129.

(23) Zhou, J.; Zhang, J.; Fang, W. H.; Yang, G. Y. A series of vanadogermanates from 1D chain to 3D framework built by Ge—V—O clusters and transition-metal-complex bridges. *Chem. Eur. J.* **2010**, 16, 13253–13261.

(24) Pitzschke, D.; Wang, J.; Hoffmann, R. D.; Pöttgen, R.; Bensch, W. Two compounds containing the mixed germanium-vanadium polyoxothioanion $[V_{14}Ge_8O_{42}S_8]_{12}$. *Angew. Chem. Int. Ed.* **2006**, 45, 1305–1308.

(25) Hu, S. Z.; Zhou, Z. H.; Robertson, B. E. Consistent approaches to Vander Waals radii for the metallic elements. *Z. Kristallogr.* **2009**, 224, 375–383.

(26) Li, H.; Eddaoudi, M.; O'Keeffe, M.; Yaghi, O. M. Design and synthesis of an exceptionally stable and highly porous metal-organic framework. *Nature* **1999**,402, 276–279.

(27) Chen, Y. M.; Wang, E. B.; Lin, B. Z.; Wang, S. T. The first polyoxoalkoxovanadium germanate anion with a novel cage-like structure: solvothermal synthesis and characterization. *Dalton Trans.* **2003**, 236, 519–520.

(28) Zhou, J.; Zhao, J. W.; Wei, Q.; Zhang, J.; Yang, G. Y. Two tetra-Cd^{II}-substituted vanadogermanate frameworks. *J. Am. Chem. Soc.* **2014**, 136, 5065–5071.

(29) Li, N.; He, D. F.; Lu, Y.; Liu, Y. W.; Li, X.; Zhong, X. H.; Guo, Z. H. A vanadogermanate dimer-based chain with magnetic and luminescent properties. *Eur. J. Inorg. Chem.* **2016**, 3143–3147.

(30) Ru, J. J.; Ma, X.; Cui, Y.; Guo, M. H.; Chen, J. Z.; Li, X. X. Two vanadogermanates from 1-dimensional chain to 2-dimensional network built from di-Cd-substituted Ge-V-O clusters and transition metal complex bridges. *Cryst. Growth Des.* **2017**, 17, 1384–1389.

(31) Akhilesh, T.; Timothy, H.; Abraham, C. The first framework solid composed of vanadosilicate clusters. *J. Am. Chem. Soc.* **2003**, 125, 10528–10529.

(32) Brown, I. D.; Altermatt, D. Bond-valence parameters obtained from a systematic analysis of the inorganic crystal structure database. *Acta Crystallogr.* **1985**, 41, 244–247.

(33) Frost, J. M.; Sanz, S.; Rajeshkumar, T.; Pitak, M. B.; Coles, S. J.; Rajaraman, G.; Wernsdorfer, W.; Schnack, J.; Lusby, P. J.; Brechin, E. K. A truncated $[Mn^{III}_{12}]$ tetrahedron from oxime-based $[Mn^{III}_3O]$ building blocks. *Dalton Trans.* **2014**, 43, 10690–10694.

(34) Wei, M. J.; Zang, H. Y.; Zhou, E. L.; Shao, K. Z.; Song, B. Q.; Wang, X. L.; Su, Z. M. Coordination and supramolecular assembly of $\{Cd_2Ge_8V_{12}O_{48}\}$ building block and cucurbit[6] to form rotaxane-shaped hybrids. *Dalton Trans.* **2016**, 45, 4989–4992.

Construction of Two Inorganic-organic Hybrid Vanadogermanates Based on Di-Cd-Substituted Ge-V-O Cluster and Transition-metal Complex Bridges

RU Jing-Jing(茹晶晶)　GU Ya-Nan(顾亚男)　MA Xiang(马祥)

CHEN Jian-Zhong(陈建中)　ZHENG Shou-Tian(郑寿添)　LI Xin-Xiong(李新雄)

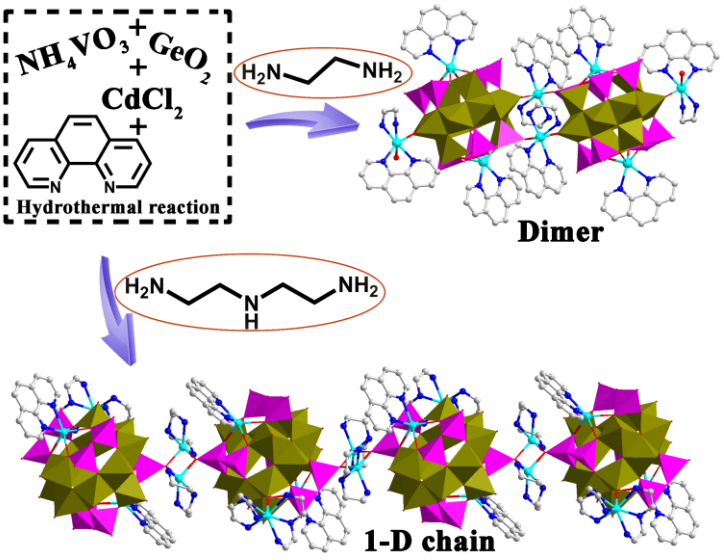

Two new inorganic-organic hybrid vanadogermanates H[Cd(en)(phen)(H_2O)][Cd(en)(phen)]{[Cd(phen)]$_2$[$Ge_8V_{12}O_{41}(OH)_7$]} 5H_2O (**1**) and [Cd(dien)$_2$][Cd(dien)]$_2${[Cd(phen)]$_2$$Ge_8V_{12}O_{42}(H_2O)(OH)_6$} 6.5$H_2O$ (**2**) (en = ethylenediamine, dien = diethylenetriamine, phen = 1,10-phenanthroline) have been synthesized by hydrothermal method. Their structures have been measured by single-crystal X-ray diffractions, thermogravimetric analysis, powder X-ray diffractions and infrared spectra.